DOI: 10.1002/chem.200601097

Anion-Directed Self-Assembly of Lanthanide–notp Compounds and Their Fluorescence, Magnetic, and Catalytic Properties

Song-Song Bao, Li-Fang Ma, Yin Wang, Ling Fang, Cheng-Jian Zhu, Yi-Zhi Li, and Li-Min Zheng*[a]

Abstract: Reactions of 1,4,7-triazacyclononane-1,4,7-triyl-tris(methylenephosphonic acid) [notpH$_6$, $C_9H_{18}N_3(PO_3H_2)_3$] with different lanthanide salts result in four types of Ln–notp compounds: $[Ln\{C_9H_{20}N_3(PO_3H)_2(PO_3)\}(NO_3)(H_2O)]\cdot 4H_2O$ (**1**), [Ln = Eu (**1Eu**), Gd (**1Gd**), Tb (**1Tb**)], $[Ln\{C_9H_{20}N_3(PO_3H)_2(PO_3)\}(H_2O)]Cl\cdot 3H_2O$ (**2**) [Ln = Eu (**2Eu**), Gd (**2Gd**), Tb (**2Tb**)], $[Ln\{C_9H_{20}N_3(PO_3H)_2(PO_3)\}(H_2O)]ClO_4\cdot 8H_2O$, (**3**) [Ln = Eu (**3Eu**), Gd (**3Gd**)], and $[Ln\{C_9H_{20}N_3(PO_3H)_2(PO_3)\}(H_2O)]ClO_4\cdot 3H_2O$ (**4**), [Ln = Gd (**4Gd**), Tb (**4Tb**)]. Compounds within each type are isostructural. In compounds **1**, dimers of $\{Ln_2(notpH_4)_2(NO_3)_2(H_2O)_2\}$ are found, in which the two lanthanide atoms are connected by two pairs of O-P-O and one pair of μ-O bridges. The NO_3^- ion serves as a bidentate terminal ligand. Compounds **2** contain similar dimeric units of $\{Ln_2(notpH_4)_2(H_2O)_2\}$ that are further connected by a pair of O-P-O bridges into an alternating chain. The Cl^- ions are involved in the interchain hydrogen-bonding networks. A similar chain structure is also found in compounds **3**; in this case, however, the chains are linked by ClO_4^- counterions through hydrogen-bonding interactions, forming an undulating layer in the (011) plane. These layers are fused through hydrogen-bonding interactions, leading to a three-dimensional supramolecular network with large channels in the [100] direction. Compounds **4** show an interesting brick-wall-like layer structure in which the neighboring lanthanide atoms are connected by a pair of O-P-O bridges. The ClO_4^- counterions and the lattice water molecules are between the layers. In all compounds the triazamacrocyclic nitrogen atoms are not coordinated to the Ln^{III} ions. The anions and the pH are believed to play key roles in directing the formation of a particular structure. The fluorescence spectroscopic properties of the Eu and Tb compounds, magnetic properties of the Gd compounds, and the catalytic properties of **4Gd** were also studied.

Keywords: lanthanides · macrocycles · organophosphonate

Introduction

Lanthanide complexes of polyazacycles with coordinating pendant arms are currently of great interest because of their potential use in applications such as magnetic resonance imaging contrast agents,[1] luminescence probes,[2] and catalysis[3], among others. So far, researches have been focused on tetraazamacrocycle derivatives with acetate side chains[4] and, more recently, those with methylenephosphinate or methylenephosphonate pendant arms,[5] owing to their strong coordination capabilities and higher selectivities toward di- and trivalent metal ions. In contrast to the tetraazamacrocycle derivatives, far less attention has been paid to the triazamacrocycle derivatives, especially those with methylenephosphonate pendant arms.[6]

A triazamacrocycle with three nitrogen-attached pendant donors is ideally suited to form six-coordinate complexes with two groups of facial donors: the macrocyclic nitrogen atoms on the one side and the pendant donors on the other. Based on 1,4,7-triazacyclononane-1,4,7-triyl-tris(methylenephosphonic acid) (notpH$_6$, $C_9N_3H_{18}(PO_3H_2)_3$), four compounds have so far been crystallographically characterized, including Fe(notpH$_3$)[7] and Cu(notpH$_4$)·H$_2$O[8] with mononuclear structures, and $Mn_3(notp)(H_2O)_6\cdot 1.5H_2O$ and $UO_2(notpH_4)\cdot H_2O$[9] with polymeric layer structures. In both Fe(notpH$_3$) and $Mn_3(notp)(H_2O)_6\cdot 1.5H_2O$, the metal ion is octahedrally surrounded by three N and three O donors. In

[a] S.-S. Bao, L.-F. Ma, Y. Wang, L. Fang, Prof. Dr. C.-J. Zhu, Prof. Dr. Y.-Z. Li, Prof. Dr. L.-M. Zheng
State Key Laboratory of Coordination Chemistry
School of Chemistry and Chemical Engineering
Nanjing University, Nanjing 210093 (PR China)
Fax: (+86) 25-8331-4502
E-mail: lmzheng@netra.nju.edu.cn

Supporting information for this article is available on the WWW under http://www.chemeurj.org/ or from the author.

 © 2007 Wiley-VCH Verlag GmbH & Co. KGaA, Weinheim

compound $Cu(notpH_4)\cdot H_2O$, the Cu^{II} ion is five-coordinate and is wrapped by three N and two phosphonate oxygen atoms from two pendant arms. In compound $UO_2(notpH_4)\cdot H_2O$, each uranyl unit is coordinated by five phosphonate oxygen atoms in the equatorial plane to yield a $\{UO_7\}$ pentagonal bipyramid. The macrocyclic nitrogen atoms are not coordinated to the metal atom.

The lanthanide ions usually have coordination numbers larger than six. When $notpH_6$ react with the lanthanide ions, there are at most nine phosphonate oxygen atoms that could be involved in coordination with the metal ions. So far some work has been carried out on the solution properties of gadolinium–notp compounds as enhancing contrast in magnetic resonance imaging.[10] While none of the structures of the lanthanide–notp compounds has been determined, the hypothetical structure of the gadolinium–notp compound in aqueous solution is supposed to be mononuclear, similar to the mononuclear lanthanide–tcta ($tctaH_3$ = 1,4,7-triazacyclononane-*N,N′,N″*-triacetate acid) compounds.[11] Considering that $notp^{6-}$ has nine phosphonate oxygen atoms as well as three macrocyclic nitrogen atoms, the coordination between the lanthanide ion and $notp^{6-}$ in solution could be more complex. Hence, it is important to investigate the structures of these Ln–notp compounds in order to better understand their structure/property relationships.

In this paper, we present the formation of four types of Ln–notp compounds in the presence of different anions at low pH. Their structures range from discrete dimers, to one-dimensional chains and two-dimensional layers. The fluorescence, magnetic, and catalytic properties of these compounds are discussed.

Results and Discussion

Syntheses: Compounds **1**, **2**, **3**, and **4** are obtained by the reactions of $notpH_6$ with different lanthanide salts in solution at room temperature. When $notpH_6$ react with lanthanide nitrates at pH 1.0–1.8, compounds **1** are formed. A higher pH leads to a turbid solution. Different molar ratios of $Ln(NO_3)_3$:$notpH_6$ (1:1, 2:1, 3:1) under the same reaction conditions result in the same compound but with different yields. The best yields are achieved at a 3:1 ratio, while crystals suitable for single-crystal X-ray diffraction measurements are obtained at a 1:1 ratio.

When $notpH_6$ react with lanthanide chlorides at pH 0.8–1.5, compounds **2** are formed in water/methanol solution. Again, the solution is turbid at higher pH values. Good yields are achieved at the $LnCl_3$:$notpH_6$ ratio of 3:1, while crystals suitable for single-crystal X-ray diffraction are obtained at a ratio of 1:1. Efforts to produce compounds **2** in an aqueous solution were not successful.

When $notpH_6$ react with lanthanide perchlorides $Ln(ClO_4)_3$ at pH 1.0–1.8, compounds **3Eu** and **4Tb** can be obtained as pure phases. However, the formation of compounds **3Gd** and **4Gd** is sensitive to pH. They can be prepared only when the pH of the reactant mixture is 1.5–1.8 and 1.0–1.2, respectively. When the pH is adjusted to 1.2–1.5, a mixture of **3Gd** and **4Gd** is obtained.

Description of crystal structures: Based on the XRD measurements, compounds of each type are isostructural (Supporting Information). Therefore, compounds **1Gd**, **2Gd**, **3Eu**, **4Gd**, and **4Tb** were selected for single crystal structural analyses. The crystallographic data for all five compounds are given in Table 1, and selected bond lengths and angles

Table 1. Crystallographic data for compounds **1Gd**, **2Gd**, **3Eu**, **4Gd**, and **4Tb**.

	1Gd	**2Gd**	**3Eu**	**4Gd**	**4Tb**
formula	$C_{18}H_{64}N_8P_6O_{34}Gd_2$	$C_9H_{30}N_3P_3O_{13}ClGd$	$C_{18}H_{80}N_6P_6O_{44}Cl_2Eu_2$	$C_9H_{28}N_3P_3O_{16}ClGd$	$C_9H_{30}N_3P_3O_{17}ClTb$
M	1437.09	673.97	1645.52	719.95	739.64
crystal dimensions [mm]	0.2×0.2×0.15	0.3×0.15×0.15	0.3×0.28×0.26	0.4×0.3×0.3	0.35×0.25×0.25
crystal system	monoclinic	monoclinic	triclinic	triclinic	triclinic
space group	$P2_1/c$	$P2_1/c$	$P\bar{1}$	$P\bar{1}$	$P\bar{1}$
a [Å]	10.926(1)	9.9662(3)	9.832(4)	9.176(2)	9.154(2)
b [Å]	13.226(1)	13.5579(4)	15.181(6)	9.251(2)	9.224(2)
c [Å]	17.024(2)	18.4269(3)	22.335(9)	15.284(3)	15.158(4)
α [°]			107.002(7)	88.369(4)	88.000(4)
β [°]	108.433(4)	116.197(1)	96.121(8)	75.816(4)	76.268(4)
γ [°]			104.096(7)	76.304(4)	75.944(4)
V [Å^3]	2334.0(4)	2234.1(1)	3035(2)	1221.5(4)	1205.7(5)
Z	2	4	2	2	2
ρ_{calcd} [g cm^{-3}]	2.045	2.004	1.801	1.957	2.037
μ [mm^{-1}]	3.134	3.368	2.400	3.096	3.324
$F(000)$	1436	1340	1664	714	736
R_{int}	0.0481	0.0215	0.0316	0.0309	0.0267
T_{max}, T_{min}	0.791, 0.733	0.603, 0.551	0.536, 0.492	0.395, 0.341	0.436, 0.384
GoF on F^2	0.995	1.121	1.139	1.034	1.077
R_1,wR_2[a] [$I>2\sigma(I)$]	0.0493, 0.1172	0.0445, 0.0984	0.0591, 0.1257	0.0591, 0.1336	0.0590, 0.1241
R_1,wR_2 (all data)	0.0623, 0.1218	0.0574, 0.1017	0.0878, 0.1314	0.0728, 0.1368	0.0704, 0.1271
$(\Delta\rho)_{max}$, $(\Delta\rho)_{min}$ [e Å^{-3}]	0.723, −1.531	0.492, −0.983	1.309, −2.392	1.235, −1.621	1.173, −1.126

[a] $R_1 = \Sigma||F_o|-|F_c||/\Sigma|F_o|$; $wR_2 = [\Sigma w(F_o^2-F_c^2)^2/\Sigma w(F_o^2)^2]^{1/2}$.

 © 2007 Wiley-VCH Verlag GmbH & Co. KGaA, Weinheim

are gathered in Tables 2–6 for **1Gd**, **2Gd**, **3Eu**, **4Gd**, and **4Tb**, respectively.

[Gd{$C_9N_3H_{20}(PO_3H)_2(PO_3)$}$(NO_3)(H_2O)$]·4$H_2O$ (***1Gd***): Compound **1Gd** crystallizes in the monoclinic space group $P2_1/c$. The asymmetric unit consists of one Gd^{3+} ion, one notpH_4^{2-} ion, one NO_3^- ion, and one coordinated and four lattice water molecules. The compound has a dinuclear molecular structure in which the two crystallographically equivalent Gd^{3+} ions are connected by two pairs of O-P-O and one pair of μ-O bridges (Figure 1). Each Gd atom is nine-coordinate with four positions occupied by phosphonate oxygen atoms O1, O2, O4, and O7 from the same notpH_4^{2-} ligand, two positions by phosphonate oxygen atoms O1A and O6A from the equivalent notpH_4^{2-} ligand, two positions by oxygen atoms O10 and O11 from the NO_3^- anion, and the remaining site filled by a water molecule (O1W). The average Gd–O distance is 2.469(4) Å (Table 2), the longest bond [2.783(4) Å] involves the terminal NO_3^- ligand.

Table 2. Selected bond lengths [Å] and angles [°] for compound **1Gd**.[a]

Gd1–O1	2.589(4)	P1–O1	1.528(5)
Gd1–O1A	2.323(5)	P1–O2	1.512(5)
Gd1–O2	2.400(4)	P1–O3	1.505(4)
Gd1–O4	2.477(4)	P2–O4	1.523(5)
Gd1–O6A	2.430(4)	P2–O5	1.570(5)
Gd1–O7	2.336(5)	P2–O6	1.509(5)
Gd1–O10	2.783(4)	P3–O7	1.493(5)
Gd1–O11	2.484(4)	P3–O8	1.561(5)
Gd1–O1W	2.398(3)	P3–O9	1.516(5)
O1A-Gd1-O2	127.30(15)	O6A-Gd1-O4	139.92(14)
O7-Gd1-O2	73.88(16)	O1W-Gd1-O4	81.49(11)
O1A-Gd1-O6A	79.56(16)	O1A-Gd1-O1	69.94(16)
O1A-Gd1-O1W	79.72(14)	O7-Gd1-O1	119.13(15)
O7-Gd1-O1W	75.46(14)	O2-Gd1-O1	57.87(15)
O2-Gd1-O1W	149.30(13)	O6A-Gd1-O1	70.16(14)
O6A-Gd1-O1W	127.81(12)	O1W-Gd1-O1	141.33(13)
O1A-Gd1-O4	80.30(14)	O4-Gd1-O1	70.47(13)
O7-Gd1-O4	73.89(15)	O11-Gd1-O10	47.66(15)
O2-Gd1-O4	88.67(14)		

[a] Symmetry transformations used to generate equivalent atoms: A: $-x+1, -y, -z$.

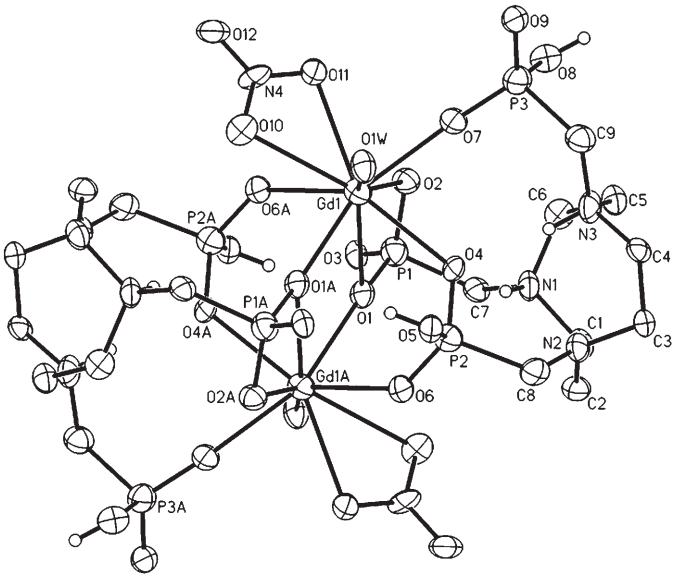

Figure 1. Dimeric structure of **1Gd** with atomic labeling scheme (thermal ellipsoids shown at 50% probability). The H atoms attached to the C atoms are omitted for clarity.

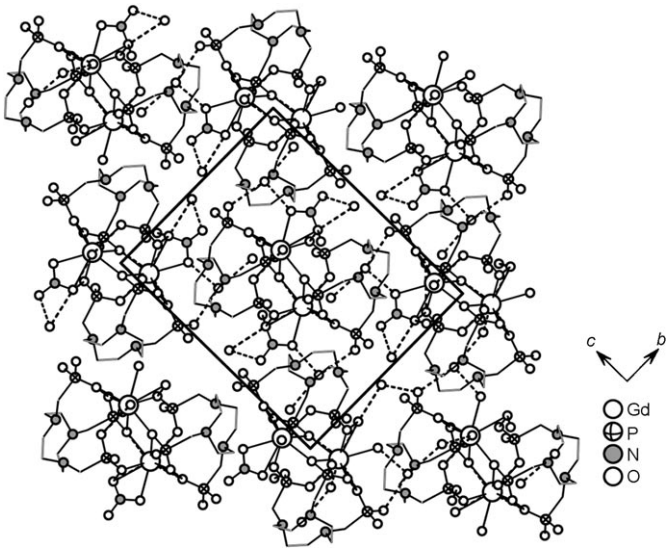

Figure 2. Structure **1Gd** packed along the [100] direction. All H atoms are omitted for clarity.

The notpH_4^{2-} in **1Gd** behaves as a zwitterionic pentadentate ligand by donating five phosphonate oxygen atoms [O1, O2, O4, O6, O7] to coordinate with the Gd^{3+} ions (Scheme 1a). The O1 atom serves as a μ_3-O and links the equivalent Gd^{3+} ions, forming a dinuclear structure containing both O-P-O and μ_3-O bridges. The Gd1···Gd1A distance is 4.028 Å. Two triazamacrocyclic nitrogen (N1 and N3) atoms and two phosphonate oxygen atoms (O5, O8) are protonated. The remaining phosphonate oxygen atoms (O3, O9) are pendant. These atoms along with the water molecules are involved in the inter- or intradimer hydrogen-bonding networks (Figure 2).

[Gd{$C_9N_3H_{20}(PO_3H)_2(PO_3)$}$(H_2O)$]Cl·3$H_2O$ (***2Gd***): Compound **2Gd** crystallizes in the monoclinic space group $P2_1/c$. The asymmetric unit is made up of one Gd^{3+} ion, one notpH_4^{2-} ion, one Cl^- ion, and one coordinated and three lattice water molecules. The structure contains a dimeric unit of $[Gd_2(notpH_4)_2(H_2O)_2]^{2+}$ which is identical to that in **1Gd** (Figure 3). In this case however, each Gd atom is eight-coordinate. Six positions are occupied by phosphonate oxygen atoms O1, O2, O4, O7, O1A and O6A from the two equivalent notpH_4^{2-} ligands, and one site by a water molecule (O1w). The remaining position is filled with the phosphonate oxygen O9B from the neighboring dimer. Accordingly, the $[Gd_2(notpH_4)_2(H_2O)_2]^{2+}$ dimers are doubly connected by the O7-P3-O9 units, forming an infinite chain

 © 2007 Wiley-VCH Verlag GmbH & Co. KGaA, Weinheim

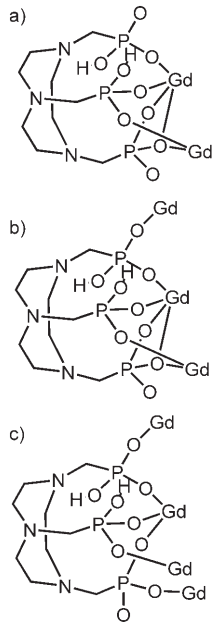

Scheme 1. Binding modes of $notpH_4^{2-}$ with two, three, and four Gd^{3+} ions.

along the *a* axis (Figure 4). The Gd–O bond lengths are between 2.348(5) and 2.666(5) Å (Table 3). The Gd···Gd distances over the μ_3-O and O-P-O bridges within the chain are 4.150 and 6.119 Å, respectively. The $notpH_4^{2-}$ serves as a hexadentate ligand using six of its nine phosphonate oxygen atoms (O1, O2, O4, O6, O7, O9) (Scheme 1b). Two triazamacrocyclic nitrogen (N1 and N3) and two phosphonate oxygen atoms (O5, O8) are again protonated. The remaining phosphonate oxygen atom (O3) is pendant. Unlike **1Gd**, in which the NO_3^- also chelates to the Gd atom, the Cl^- in **2Gd** is not coordinated; instead, it is involved in the hydrogen-bonding networks (Figure 5).

Table 3. Selected bond lengths [Å] and angles [°] for compound **2Gd**.[a]

Gd1–O1	2.666(5)	P1–O1	1.528(5)
Gd1–O1A	2.348(5)	P1–O2	1.522(5)
Gd1–O2	2.413(4)	P1–O3	1.520(4)
Gd1–O4	2.460(4)	P2–O4	1.532(4)
Gd1–O6A	2.382(4)	P2–O5	1.551(4)
Gd1–O7	2.353(4)	P2–O6	1.498(4)
Gd1–O9B	2.375(4)	P3–O7	1.492(5)
Gd1–O1W	2.416(4)	P3–O8	1.544(4)
		P3–O9	1.501(4)
O1A-Gd1-O7	141.73(15)	O2-Gd1-O1W	81.90(14)
O1A-Gd1-O9B	79.02(13)	O1A-Gd1-O4	78.53(14)
O7-Gd1-O9B	79.04(13)	O7-Gd1-O4	73.41(14)
O1A-Gd1-O6A	74.20(14)	O9B-Gd1-O4	96.83(14)
O8-Gd1-O6A	142.54(13)	O8A-Gd1-O4	139.66(13)
O9B-Gd1-O6A	106.36(13)	O2-Gd1-O4	87.77(13)
O1A-Gd1-O2	125.74(15)	O1W-Gd1-O4	149.77(13)
O7-Gd1-O2	78.97(15)	O1A-Gd1-O1	68.42(16)
O9B-Gd1-O2	155.19(14)	O7-Gd1-O1	123.84(14)
O6A-Gd1-O2	84.68(14)	O9B-Gd1-O1	146.87(13)
O1A-Gd1-O1W	130.09(14)	O6A-Gd1-O1	71.12(13)
O7-Gd1-O1W	76.74(13)	O2-Gd1-O1	57.47(15)
O9B-Gd1-O1W	82.00(13)	O1W-Gd1-O1	123.75(14)
O6A-Gd1-O1W	67.68(13)	O4-Gd1-O1	71.45(13)

[a] Symmetry transformations used to generate equivalent atoms: A: $-x+1, -y+1, -z+2$; B: $-x+2, -y+1, -z+2$.

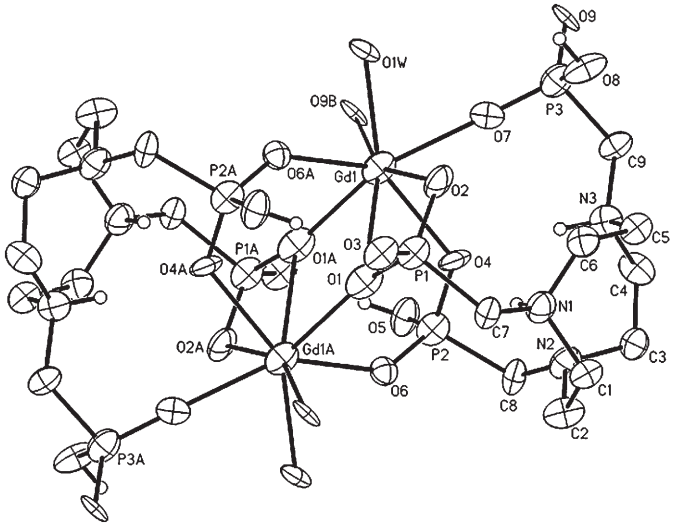

Figure 3. Building unit of structure **2Gd** with atomic labeling scheme (thermal ellipsoids shown at 50% probability). The H atoms attached to the C atoms are omitted for clarity.

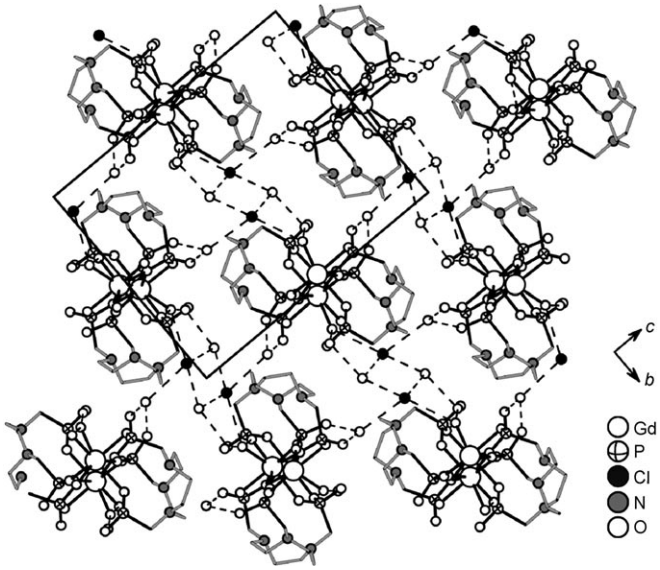

Figure 5. Structure **2Gd** packed along the [100] direction. All H atoms are omitted for clarity.

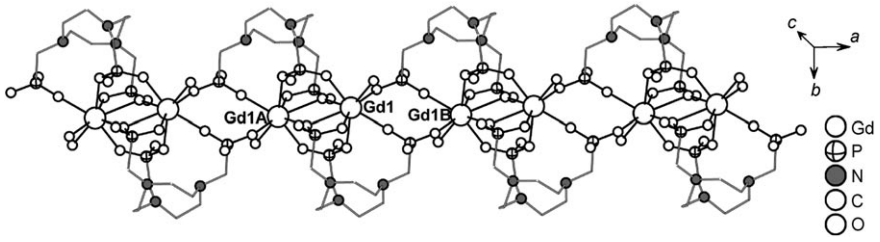

Figure 4. One chain of structure **2Gd** running along the *a* axis.

$[Eu\{C_9N_3H_{20}(PO_3H)_2(PO_3)\}(H_2O)]ClO_4\cdot 8H_2O$ (***3Eu***): Compound **3Eu** crystallizes in the triclinic space group $P\bar{1}$. The asymmetric unit contains two independent Eu^{3+} ions, two $notpH_4^{2-}$ ions, two ClO_4^- ions, and two coordinated and sixteen lattice water molecules. The coordination geometries

 © 2007 Wiley-VCH Verlag GmbH & Co. KGaA, Weinheim

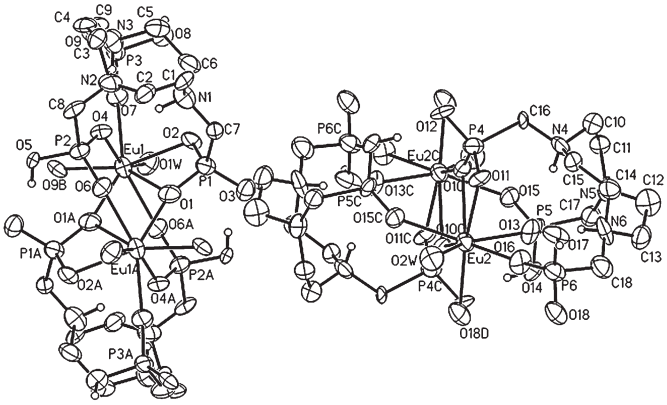

Figure 6. Building unit of structure **3Eu** with atomic labeling scheme (thermal ellipsoids shown at 50% probability). The H atoms attached to the C atoms are omitted for clarity.

Table 4. Selected bond lengths [Å] and angles [°] for compound **3Eu**.[a]

Eu1–O1	2.634(5)	Eu2–O10	2.639(5)
Eu1–O1A	2.358(5)	Eu2–O10C	2.331(5)
Eu1–O2	2.387(4)	Eu2–O11	2.423(5)
Eu1–O4	2.487(5)	Eu2–O13	2.472(5)
Eu1–O6A	2.359(4)	Eu2–O15C	2.394(5)
Eu1–O7	2.331(4)	Eu2–O16	2.353(4)
Eu1–O9B	2.362(4)	Eu2–O18D	2.320(5)
Eu1–O1W	2.401(5)	Eu2–O2W	2.465(5)
P1–O1	1.518(5)	P4–O10	1.548(5)
P1–O2	1.526(4)	P4–O11	1.481(4)
P1–O3	1.521(5)	P4–O12	1.519(4)
P2–O4	1.489(5)	P5–O13	1.494(4)
P2–O5	1.570(4)	P5–O14	1.557(5)
P2–O6	1.486(4)	P5–O15	1.474(5)
P3–O7	1.479(5)	P6–O16	1.464(5)
P3–O8	1.586(5)	P6–O17	1.548(5)
P3–O9	1.480(5)	P6–O18	1.498(6)
O7-Eu1-O1A	142.81(17)	O18D-Eu2-O10C	79.49(17)
O7-Eu1-O6A	141.47(17)	O18D-Eu2-O16	81.50(18)
O1A-Eu1-O6A	74.50(16)	O10C-Eu2-O16	142.42(17)
O7-Eu1-O9B	81.38(15)	O18D-Eu2-O15C	104.72(17)
O1A-Eu1-O9B	77.77(16)	O10C-Eu2-O15C	75.36(16)
O6A-Eu1-O9B	105.79(15)	O16-Eu2-O15C	141.25(17)
O7-Eu1-O2	76.45(15)	O18D-Eu2-O11	154.76(16)
O1A-Eu1-O2	127.14(15)	O10C-Eu2-O11	125.74(14)
O6A-Eu1-O2	85.22(16)	O16-Eu2-O11	77.63(16)
O9B-Eu1-O2	155.04(14)	O15C-Eu2-O11	83.54(16)
O7-Eu1-O1W	76.45(18)	O18D-Eu2-O2W	81.19(19)
O1A-Eu1-O1W	130.31(16)	O10C-Eu2-O2W	132.35(18)
O6A-Eu1-O1W	67.16(16)	O16-Eu2-O2W	75.32(18)
O9B-Eu1-O1W	83.38(17)	O15C-Eu2-O2W	68.18(18)
O2-Eu1-O1W	80.43(17)	O11-Eu2-O2W	79.93(16)
O7-Eu1-O4	73.99(16)	O18D-Eu2-O13	98.53(18)
O1A-Eu1-O4	78.44(14)	O10C-Eu2-O13	77.87(15)
O6A-Eu1-O4	139.48(14)	O16-Eu2-O13	73.29(15)
O9B-Eu1-O4	97.14(16)	O15C-Eu2-O13	140.30(14)
O2-Eu1-O4	87.72(16)	O11-Eu2-O13	88.94(17)
O1W-Eu1-O4	149.98(16)	O2W-Eu2-O13	148.27(16)
O7-Eu1-O1	122.32(15)	O18D-Eu2-O10	147.59(16)
O1A-Eu1-O1	69.21(18)	O10C-Eu2-O10	68.38(16)
O6A-Eu1-O1	71.53(14)	O16-Eu2-O10	122.04(16)
O9B-Eu1-O1	146.43(15)	O15C-Eu2-O10	71.83(15)
O2-Eu1-O1	58.07(14)	O11-Eu2-O10	57.57(13)
O1W-Eu1-O1	122.80(16)	O2W-Eu2-O10	123.80(17)
O4-Eu1-O1	70.94(15)	O13-Eu2-O10	71.29(14)

[a] Symmetry transformations used to generate equivalent atoms: A: $-x+1, -y, -z$; B: $-x+2, -y, -z$; C: $-x+1, -y, -z+1$; D: $-x, -y, -z+1$.

around the Eu atoms are identical to that in **2Gd** (Figure 6). Each Eu atom is linked by the phosphonate oxygen atoms from $notpH_4^{2-}$, forming two types of chains along the *a* axis. Each type of chain contains dimeric units of $[Eu_2(notpH_4)_2(H_2O)_2]^{2+}$ doubly connected by the O-P-O groups, which is very similar to the chain observed in **2Gd**. The Eu–O bond lengths fall in the range of 2.320(5)–2.639(5) Å (Table 4), comparable to those in **2Gd**. The significant difference between structures **2Gd** and **3Eu** lies in the packing of these chains within the lattice. In **3Eu**, four neighboring chains are linked by the ClO_4^- ions through hydrogen bonding, forming a supramolecular network structure with large channels along the [100] direction. A large number of lattice water molecules reside within the channels (Figure 7).

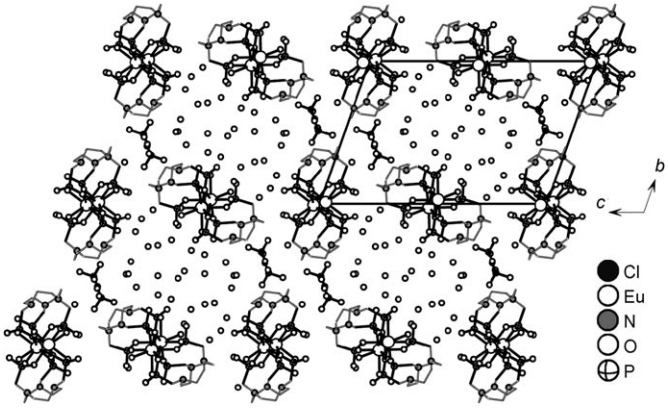

Figure 7. Structure **3Eu** packed along the *a* axis. All H atoms are omitted for clarity.

$[Gd\{C_9N_3H_{20}(PO_3H)_2(PO_3)\}(H_2O)]ClO_4{\cdot}3H_2O$ ***(4Gd)***: Compound **4Gd** crystallizes in the triclinic space group $P\bar{1}$. The asymmetric unit contains one independent Gd^{3+} ion, one $notpH_4^{2-}$ ion, one ClO_4^- ion, and one coordinated and three lattice water molecules. The Gd atom is seven-coordinate and has a distorted pentagonal-bipyramidal geometry, with three phosphonate oxygens (O1, O4 and O7) from the same $notpH_4^{2-}$ ligand, three phosphonate oxygens (O2A, O6B and O8C) from the other three $notpH_4^{2-}$ ligands, and one oxygen from the water molecule (Figure 8). The Gd–O bond lengths are in the range of 2.245(5)–2.510(6) Å.

The $notpH_4^{2-}$ is also hexadentate by using six of its nine phosphonate oxygen atoms (Scheme 1c). It chelates to the same Gd^{3+} ion through phosphonate oxygen atoms O1, O4 and O7, forming a mononuclear unit of $[Gd(notpH_4)]^+$. This unit behaves as a tridentate "ligand" and links to three Gd atoms from the other units with phosphonate oxygen atoms O2, O6 and O8. Consequently, the $\{GdO_7\}$ and $\{CPO_3\}$ polyhedra are connected by corner sharing, forming a two-dimensional inorganic brick-wall-like layer structure containing 24-member rings. The coordinated water molecules point toward the center of the rings (Figure 9). Two triazamacrocyclic nitrogen atoms (N1 and N3) and two phosphonate oxygen atoms (O3, O5) of $notpH_4^{2-}$ are protonated.

 © 2007 Wiley-VCH Verlag GmbH & Co. KGaA, Weinheim

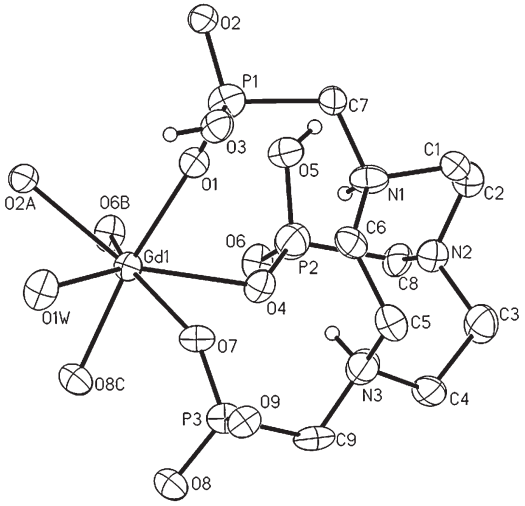

Figure 8. Building unit of structure **4Gd** with atomic labeling scheme (thermal ellipsoids shown at 50% probability). The H atoms attached to the C atoms are omitted for clarity.

Table 5. Selected bond lengths [Å] and angles [°] for compound **4Gd**.[a]

Gd1−O1	2.294(6)	P1−O2	1.487(6)
Gd1−O2A	2.327(5)	P1−O3	1.541(6)
Gd1−O4	2.463(5)	P2−O4	1.509(6)
Gd1−O6B	2.279(5)	P2−O5	1.560(6)
Gd1−O7	2.305(5)	P2−O6	1.494(6)
Gd1−O8C	2.245(5)	P3−O7	1.490(5)
Gd1−O1W	2.510(6)	P3−O8	1.503(6)
P1−O1	1.475(6)	P3−O9	1.527(5)
O8C-Gd1-O6B	80.7(2)	O8C-Gd1-O4	96.5(2)
O8C-Gd1-O1	171.6(2)	O6B-Gd1-O4	77.11(18)
O6B-Gd1-O1	105.6(2)	O1-Gd1-O4	79.79(19)
O8C-Gd1-O7	88.3(2)	O7-Gd1-O4	74.81(18)
O6B-Gd1-O7	148.39(19)	O2A-Gd1-O4	141.36(18)
O1-Gd1-O7	83.45(19)	O8C-Gd1-O1W	83.9(2)
O8C-Gd1-O2A	104.4(2)	O6B-Gd1-O1W	135.82(19)
O6B-Gd1-O2A	74.7(2)	O1-Gd1-O1W	95.0(2)
O1-Gd1-O2A	82.87(19)	O7-Gd1-O1W	71.23(19)
O7-Gd1-O2A	136.9(2)	O2A-Gd1-O1W	69.48(19)

[a] Symmetry transformations used to generate equivalent atoms: A: $-x+1, -y, -z+1$; B: $-x, -y, -z+1$; C: $-x, -y+1, -z+1$.

The atom O9 is pendant. The triazacyclononane moieties reside on both sides of the inorganic layer. The ClO_4^- counterions and the lattice water molecules are between the adjacent layers (Figure 10).

Compound **4Tb** is isostructural to compound **4Gd**. However, the cell volume of **4Tb** [1205.7(5) Å^3] is slightly smaller than that of **4Gd** [1221.5(4) Å^3], which is attributed to the effect of lanthanide contraction. The Tb−O bond lengths are in the range of 2.231(5)–2.511(5) Å (Table 6). Two triazamacrocyclic nitrogen atoms (N1 and N3) and two phosphonate oxygen atoms (O3, O5) of notpH_4^{2-} are also protonated.

The roles of the anions and pH: Compounds **1–4** are obtained through reactions of lanthanide salts and notpH_6 under similar experimental conditions at low pH (<2.0). Al-

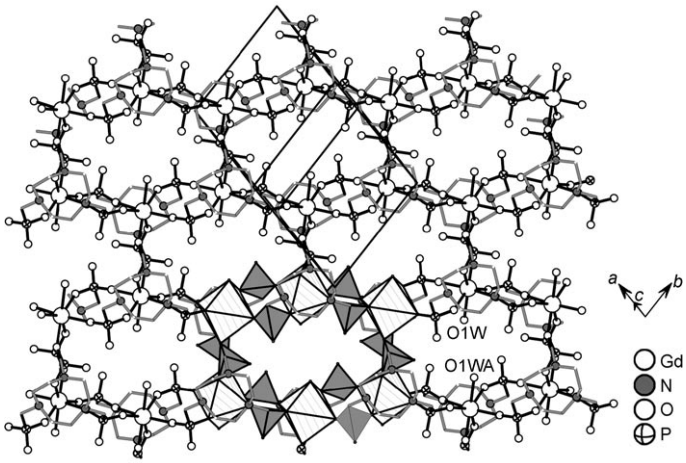

Figure 9. One layer of structure **4Gd**. All H atoms are omitted for clarity.

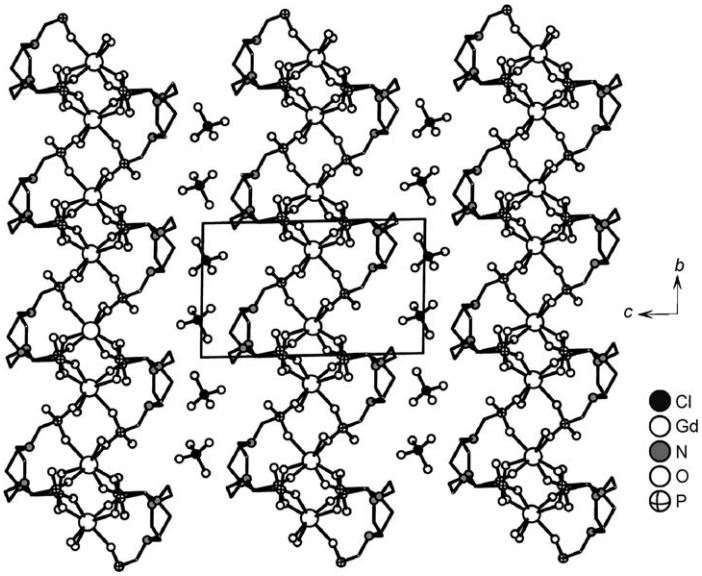

Figure 10. Packing diagram of structure **4Gd** along the *a* axis. All H atoms are omitted for clarity.

Table 6. Selected bond lengths [Å] and angles [°] for compound **4Tb**.[a]

Tb1−O1	2.247(5)	P1−O2	1.498(6)
Tb1−O3A	2.257(5)	P1−O3	1.557(5)
Tb1)−O4	2.440(5)	P2−O4	1.523(5)
Tb1−O6B	2.278(5)	P2−O5	1.569(6)
Tb1−O7	2.277(5)	P2−O6	1.473(5)
Tb1−O8C	2.231(5)	P3−O7	1.499(5)
Tb1−O1W	2.511(5)	P3−O8	1.493(5)
P1−O1	1.503(6)	P3−O9	1.524(5)
O8C-Tb1-O6B	80.85(18)	O8C-Tb1-O4	96.30(19)
O8C-Tb1-O1	172.61(18)	O6B-Tb1-O4	76.57(17)
O6B-Tb1-O1	104.58(18)	O1-Tb1-O4	80.34(18)
O8C-Tb1-O7	88.24(18)	O7-Tb1-O4	74.63(17)
O6B-Tb1-O7	147.80(18)	O3A-Tb1-O4	142.37(18)
O1-Tb1-O7	84.52(18)	O8C-Tb1-O1W	83.7(2)
O8C-Tb1-O3A	103.53(18)	O6B-Tb1-O1W	135.32(17)
O6B-Tb1-O3A	75.46(18)	O1-Tb1-O1W	95.5(2)
O1-Tb1-O3A	82.88(18)	O7-Tb1-O1W	72.38(18)
O7-Tb1-O3A	136.73(18)	O3A-Tb1-O1W	67.91(18)

[a] Symmetry transformations used to generate equivalent atoms: A: $-x+2, -y+1, -z$; B: $-x+1, -y+1, -z$; C: $-x+1, -y+2, -z$.

© 2007 Wiley-VCH Verlag GmbH & Co. KGaA, Weinheim

though they show analogous compositions with a Ln:notpH_4^{2-} molar ratio of 1:1, their structures are remarkably different from each other. In compounds **1**, the nine-coordinate Ln atoms are bridged by O-P-O and μ_3-O linkers, forming a discrete dinuclear structure. In compounds **2**, the dimeric unit of $[Ln_2(notpH_4)_2(H_2O)_2]^{2+}$ is further connected through O-P-O units into an alternating chain. Compounds **3** also show a chain structure similar to that in **2**. In this case, however, the chains are packed in such a way that large channels are generated along the *a* axis. These host a large amount of lattice water. In compounds **4**, the $\{GdO_7\}$ and $\{CPO_3\}$ polyhedra are connected by corner sharing, forming a brick-wall-like layer structure which contains 24-member rings.

The two triazamacrocyclic nitrogen and two phosphonate oxygen atoms of notpH_4^{2-} are protonated in all cases, leaving seven phosphonate oxygen and one nitrogen atoms as potential donors for coordination (Scheme 1). The structural differences in compounds **1**–**4** should mainly originate from both the coordination capability and the size of the anionic counterions. The NO_3^- ion can act as a bidentate terminal ligand, and chelates to the same Ln atom, forming a dinuclear structure as found in **1**. In compounds **2**, on the other hand, the Cl^- ion is not coordinated to the Ln atom. The vacant coordination sites of the Ln atoms are filled with phosphonate oxygen atoms from the neighboring dimmers to form an alternating chain structure. Although a similar chain structure is observed in **3**, the ClO_4^- counterions, being larger than Cl^-, fill in spaces in the neighboring four chains, resulting in a supramolecular network containing large channels. It is interesting that compounds **4** with layer structures can be obtained in the presence of the same ClO_4^- ion. In **4**, the Ln atoms are bridged purely through the O-P-O units forming an inorganic layer with the ClO_4^- ions that occupy the interlayer spaces.

Noting that compound **3Gd** is prepared at pH 1.5–1.8 whereas compound **4Gd** is obtained at pH 1.0–1.2, the pH of the reaction mixture clearly plays an important role in the formation of compounds **3Gd** and **4Gd**. Further, we also tried to prepare compounds **3Tb** or **4Eu** under the same conditions but obtained crystalline or powder phases of **4Tb** or **3Eu**, respectively. The effect of the lanthanide contraction could not be excluded.

Luminescent properties: Upon excitation at 396 nm in the solid state at room temperature, compounds **1Eu**, **2Eu**, and **3Eu** emit strong red luminescence characteristic for the Eu^{3+} ions (Table 7 and Figure 11). The emission bands appear at about 580, 590, 619, 653, and 696 nm, corresponding to the $^5D_0 \rightarrow {}^7F_n$ (n = 0–4) transitions. The $^5D_0 \rightarrow {}^7F_0$ transition at 580 nm is extremely weak, in agreement with the low-symmetry environments around the Eu atoms. The $^5D_0 \rightarrow {}^7F_1$ transition is magnetic dipole in nature and not environmentally sensitive, while the $^5D_0 \rightarrow {}^7F_2$ transition is electric dipole allowed and hypersensitive to the crystal field.[12] For the present three Eu compounds, two signals (or shoulders) are found in the $^5D_0 \rightarrow {}^7F_1$ and $^5D_0 \rightarrow {}^7F_2$ regions, but the relative intensities are different. For compounds **2Eu** and **3Eu**, the intensities of the $^5D_0 \rightarrow {}^7F_1$ and $^5D_0 \rightarrow {}^7F_2$ transitions are comparable, indicating relatively symmetric crystal fields for the two compounds. For compound **1Eu**, the intensity of the $^5D_0 \rightarrow {}^7F_2$ transition is about twice that of the $^5D_0 \rightarrow {}^7F_1$ transition.

Table 7. Emission bands for the Eu and Tb compounds.

	Observed transition [nm]				
	$^5D_0 \rightarrow {}^7F_0$	$^5D_0 \rightarrow {}^7F_1$	$^5D_0 \rightarrow {}^7F_2$	$^5D_0 \rightarrow {}^7F_3$	$^5D_0 \rightarrow {}^7F_4$
1Eu	580 (weak)	588 and 595	619	653 (weak)	696
2Eu	580 (weak)	592	613 and 620	653 (weak)	693 (weak) and 700
3Eu	579 (weak)	594	613 and 619	653 (weak)	691 (weak) and 700

	observed transition [nm]			
	$^5D_4 \rightarrow {}^7F_6$	$^5D_4 \rightarrow {}^7F_5$	$^5D_4 \rightarrow {}^7F_4$	$^5D_4 \rightarrow {}^7F_3$
1Tb	489	544	585	622
2Tb	491	545	588	621
4Tb	487	542 and 549	582 and 592	622

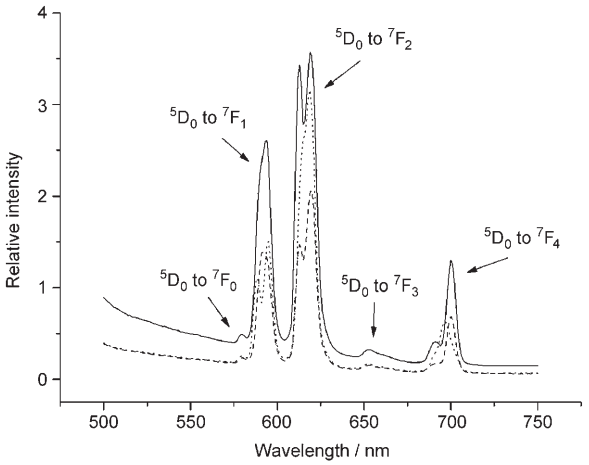

Figure 11. Emission spectra of **1Eu** (·····), **2Eu** (-----), and **3Eu** (——) in solid state (λ_{ex} = 396 nm).

Figure 12 shows the emission spectra of compounds **1Tb**, **2Tb**, and **4Tb** excited at 375 nm. The most intense transition is $^5D_4 \rightarrow {}^7F_5$, which implies green emission light characteristic for the Tb^{3+} ion.[12]

Magnetic properties: The magnetic properties of compounds **1Gd**, **2Gd**, and **4Gd** were investigated in the 1.8–300 K temperature range. Figure 13 shows the χ_M and $\chi_M T$ versus T plots for **1Gd**. The $\chi_M T$ value per Gd_2 at 300 K is 15.76 $cm^3 K mol^{-1}$, close to the theoretical value (15.75 $cm^3 K mol^{-1}$) for a binuclear complex of Gd^{3+} with spin S = $^7/_2$ and g = 2. The susceptibility data obeys the Curie–Weiss law over the whole temperature range. The Weiss constant (θ) is −0.23 K. The negative Weiss constant and the decrease of $\chi_M T$ upon cooling indicate a very weak antiferromagnetic interaction between the magnetic centers.

 © 2007 Wiley-VCH Verlag GmbH & Co. KGaA, Weinheim

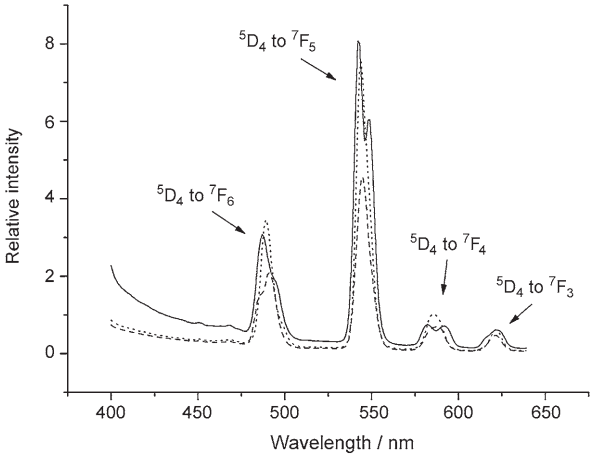

Figure 12. Emission spectra of **1Tb** (•••••), **2Tb** (-----), and **4Tb** (——) in solid state (λ_{ex} = 375 nm).

The data were analyzed by the equation[13] deduced from the isotropic spin Hamiltonian $H = -JS_{Gd1}{\cdot}S_{Gd2}$ with the quantum numbers $S_{Gd1} = S_{Gd2} = {}^7/_2$. The theoretical fitting, shown as the solid line in Figure 13, gives $J = -0.015\ cm^{-1}$ and $g = 2.0$. The small J value is comparable to that found for the other μ-O bridged Gd_2 compounds.[14]

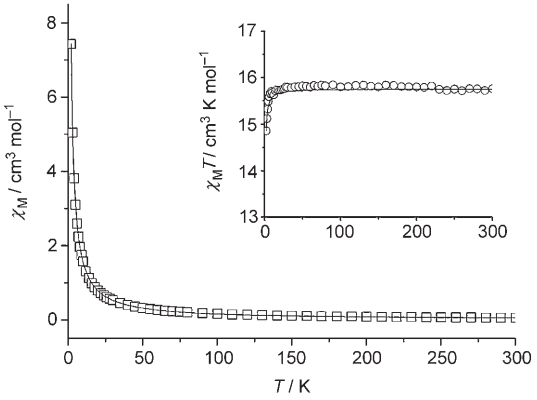

Figure 13. χ_M and $\chi_M T$ versus T plots for **1Gd**.

For **2Gd**, the $\chi_M T$ value per Gd_2 at 300 K is 15.83 $cm^3 K mol^{-1}$, in agreement with the theoretical value. The susceptibility data obeys the Curie–Weiss law over the whole temperature range with the Weiss constant (θ) +0.31 K. The positive Weiss constant as well as the continuous increasing of $\chi_M T$ upon cooling suggest a very weak ferromagnetic interaction between the Gd^{3+} ions (Figure 14). A weak ferromagnetic interaction is also observed in **4Gd**. In this case, the Weiss constant $\theta = +0.56$ K (Supporting Information).

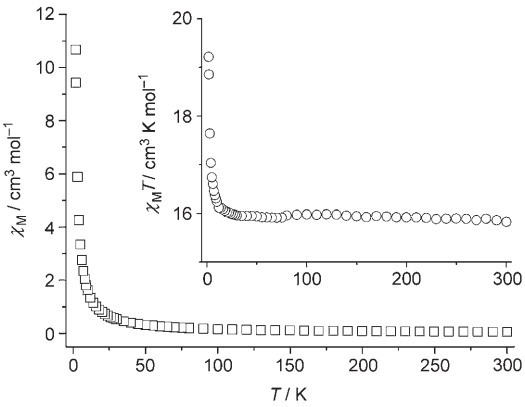

Figure 14. χ_M and $\chi_M T$ versus T plots for **2Gd**.

Catalyzed Biginelli reaction: The venerable Biginelli reaction, one-pot cyclocondensation of aldehyde, 1,3-ketoester, and urea or thiourea, is one of the most useful multicomponent reactions in organic synthesis.[15] Products of the Biginelli reaction, polyfunctionalized dihydropyrimidines, represent a heterocyclic system of remarkable pharmacological efficiency, and many exhibit antiviral, antitumor, antibacterial, and anti-inflammatory properties.[16] It has been disclosed that lanthanide triflate can efficiently catalyze the Biginelli reaction under mild conditions.[17]

As the compound **4Gd** maintained the framework structure after removal of the coordinated water molecules, we explored the Biginelli reaction using **4Gd** as the catalyst-(Scheme 2). The condensation of benzaldehyde, ethyl acetoacetate, and urea was tested in the presence of 5 mol% dehydrated compound **4Gd** employing methanol as solvent.[18] We were pleased to find that dihydropyrimidine was obtained in 60% yield after the reaction was carried out for 48 h. No product can be obtained without the presence of **4Gd**. In addition, the catalyst could easily be recovered and reused without loss of activity. Those preliminary results show that the compound **4Gd** is an effective catalyst for the Biginelli reaction.

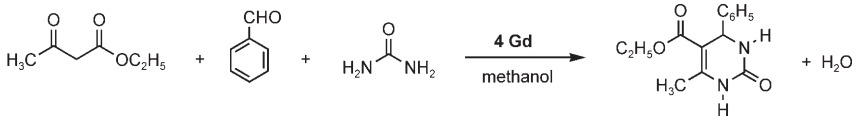

Scheme 2.

Conclusion

Four types of Ln–notp compounds can be obtained through the reactions of 1,4,7-triazacyclononane-1,4,7-triyl-tris(methylenephosphonic acid) [notpH_6, $C_9H_{18}N_3(PO_3H_2)_3$] and different lanthanide salts in solution at low pH. When lanthanide nitrates are used as the starting materials, dinuclear

 © 2007 Wiley-VCH Verlag GmbH & Co. KGaA, Weinheim

compounds $[Ln\{C_9H_{20}N_3(PO_3H)_2(PO_3)\}(NO_3)(H_2O)]\cdot 4H_2O$ **1** (Ln = Eu, Gd, Tb) result, in which the NO_3^- ion chelates the same lanthanide ion. When lanthanide chlorides are used as the starting materials, chain compounds $[Ln\{C_9H_{20}N_3(PO_3H)_2(PO_3)\}(H_2O)]Cl\cdot 3H_2O$ **2** (Ln = Eu, Gd, Tb) are produced, in which the Cl^- ions reside between the chains. It is interesting that compounds $[Ln\{C_9H_{20}N_3(PO_3H)_2(PO_3)\}(H_2O)]ClO_4\cdot 8H_2O$ **3** (Ln = Eu, Gd) with a chain structure and $[Ln\{C_9H_{20}N_3(PO_3H)_2(PO_3)\}(H_2O)]ClO_4\cdot 3H_2O$ **4** (Ln = Gd, Tb) with a layer structure can be obtained at slightly different pH by using lanthanide perchlorides as the starting materials. In both cases, the ClO_4^- ions are not coordinated to the metal ions but fill in the interchain or interlayer spaces. This result demonstrates that the coordination capability and size of the anions as well as the pH of the reaction mixture play important roles in directing the formation of Ln–notp compounds with different structures. The fluorescence spectroscopic studies show that the Eu and Tb compounds emit strong red and green luminescence characteristic for the Eu^{3+} and Tb^{3+} ions, respectively. The magnetic susceptibility measurements of the Gd compounds confirm that only very week antiferromagnetic or ferromagnetic interactions are propagated between the Gd centers. Preliminary results on the catalytic properties of compound **4Gd** show that it is an effective catalyst for the Biginelli reaction.

Experimental Section

Materials and measurements

General: 1,4,7-Triazacyclononane-1,4,7-triyl-tris(methylenephosphonic acid) ($notpH_6$) was prepared according to literature methods.[19] All the other starting materials were of reagent grade quality and were obtained from commercial sources without further purification. The elemental analyses were performed in a PE240C elemental analyzer. The infrared spectra were recorded on a VECTOR 22 spectrometer with pressed KBr pellets. Thermal analyses were performed in nitrogen in 30–800 °C the temperature range with a heating rate of 10 °C min^{-1} on a TGA-DTA V1.1b Inst 2100 instrument. The fluorescent spectra were recorded on a SHIMADZU VF-320 spectrometer with polycrystalline samples. The magnetic susceptibility data were obtained on polycrystalline samples (17.11 mg for **1Gd**, 7.84 mg for **2Gd** and 4.31 mg for **4Gd**) using a Quantum Design MPMS-XL7 SQUID magnetometer.

$[Gd\{C_9N_3H_{20}(PO_3H)_2(PO_3)\}(NO_3)(H_2O)]\cdot 4H_2O$ (1Gd): A solution of $notpH_6$ (0.05 mmol, 0.020 g) and $Gd(NO_3)_3\cdot 6H_2O$ (0.15 mmol, 0.068 g) in water (20 mL) was adjusted by addition of 1 M HNO_3 to pH 1.0. After keeping at room temperature for 2 d, colorless rhombic crystals of **1Gd** were obtained in 65% yield based on $notpH_6$. IR (KBr): $\tilde{\nu}$ = 3440–2852 (br), 2386 (m), 1664 (m), 1384 (s), 1328 (m), 1156 (s), 1142 (s), 1063 (s), 994 (m), 931 (m), 773 (m), 554 cm^{-1}(m); elemental analysis calcd (%) for $C_9H_{24}N_4P_3O_{13}Gd\cdot 4H_2O$: C 15.04, H 4.49, N 7.80; found: C 14.88, H 4.26, N 7.87; thermal analysis shows a weight loss of 12.6% in the 30–280 °C temperature range, close to the calculated value for the release of five water molecules (12.5%).

$[Eu\{C_9N_3H_{20}(PO_3H)_2(PO_3)\}(NO_3)(H_2O)]\cdot 4H_2O$ (1Eu): The preparation of this compound follows the same procedure as for **1Gd** except that $Eu(NO_3)_3$ (0.15 mmol, 0.067 g) instead of $Gd(NO_3)_3$ was used as the starting material. The colorless rhombic crystals of **1Eu** were obtained in 60% yield. IR (KBr): $\tilde{\nu}$ = 3442–2852 (br), 2345 (m), 1668 (m), 1384 (s), 1332 (m), 1158 (s), 1143 (s), 1064 (s), 996 (m), 932 (m), 775 (m), 556 cm^{-1}(m); elemental analysis calcd (%) for $C_9H_{24}N_4P_3O_{13}Eu\cdot 4H_2O$: C 15.16, H 4.52, N 7.86; found: C 14.42, H 4.81, N 7.48; thermal analysis shows that the weight loss in the 30–260 °C temperature range is 12.3%, close to the calculated value for the release of five water molecules (12.6%).

$[Tb\{C_9N_3H_{20}(PO_3H)_2(PO_3)\}(NO_3)(H_2O)]\cdot 4H_2O$ (1Tb): The preparation of this compound follows the same procedure as for **1Gd** except that $Tb(NO_3)_3$ (0.15 mmol, 0.068 g) instead of $Gd(NO_3)_3$ was used as the starting material. The colorless rhombic crystals of **1Tb** were obtained in 70% yield. IR (KBr): $\tilde{\nu}$ = 3431–2856 (br), 2358 (w), 1666 (m), 1384 (s), 1325 (m), 1160 (s), 1140 (s), 1064 (s), 994 (m), 928 (m), 768 (m), 553 (m), 488 cm^{-1}(m); elemental analysis calcd (%) for $C_9H_{24}N_4P_3O_{13}Tb\cdot 4H_2O$: C 15.01, H 4.48, N 7.78; found: C 14.64, H 4.76, N 7.37; thermal analysis reveals that the weight loss in the 30–270 °C temperature range is 11.9%, close to the calculated value for the release of five water molecules (12.5%).

$[Gd\{C_9N_3H_{20}(PO_3H)_2(PO_3)\}(H_2O)]Cl\cdot 3H_2O$ (2Gd): A solution of $notpH_6$ (0.05 mmol, 0.020 g) and $(CH_3)_4NOH$ (0.05 mmol, 0.0045 g) in water-methanol (5 mL/5 mL) was added to a solution of $GdCl_3\cdot 6H_2O$ (0.15 mmol, 0.055 g) in water (5 mL). The 1 M HCl was dropped into the mixture until the solution became clear (pH ≈ 1). The clear solution was left at room temperature for a week to afford colorless prismatic crystals of **2Gd** in 65% yield based on $notpH_6$. IR(KBr): $\tilde{\nu}$ = 3385–2870 (br), 1626 (w), 1182 (s), 1112 (m), 1042 (m), 919 (m), 771 (w), 556 cm^{-1} (m); elemental analysis calcd (%) for $C_9H_{24}N_3P_3O_{10}ClGd\cdot 3H_2O$: C 16.03, H 4.49, N 6.23; found: C 16.19, H 4.54, N 6.08; thermal analysis shows a weight loss of 11.1% in the 50–143 °C temperature range, close to the calculated value for the release of four water molecules (10.7%).

$[Eu\{C_9N_3H_{20}(PO_3H)_2(PO_3)\}(H_2O)]Cl\cdot 3H_2O$ (2Eu): The preparation of this compound follows the same procedure as for **2Gd** except that $EuCl_3$ (0.15 mmol, 0.055 g) was used as the starting material instead of $GdCl_3$. The colorless prismatic crystals of **2Eu** were obtained in 68% yield. IR (KBr): $\tilde{\nu}$ = 3395–2869 (br), 1627 (w), 1180 (s), 1141 (m), 1111 (s), 1043 (m), 918 (m), 770 (w), 551 cm^{-1} (m); elemental analysis calcd (%) for $C_9H_{24}N_3P_3O_{10}ClEu\cdot 3H_2O$: C 16.16, H 4.52, N 6.28; found: C 15.74, H 4.52, N 6.36; thermal analysis shows a weight loss of 11.3% in the 50–143 °C temperature range, close to the calculated value for the release of four water molecules (10.8%).

$[Tb\{C_9N_3H_{20}(PO_3H)_2(PO_3)\}(H_2O)]Cl\cdot 3H_2O$ (2Tb): The preparation of this compound follows the same procedure as for **2Gd** except that $TbCl_3$ (0.15 mmol, 0.056 g) was used as the starting material instead of $GdCl_3$. The colorless prismatic crystals of **2Tb** were obtained in 73% yield. IR (KBr): $\tilde{\nu}$ = 3406–2867 (br), 1636 (w), 1159 (m), 1140 (s), 1112 (m), 1090 (s), 1050 (m), 1029 (m), 922 (w), 770 (w), 549 cm^{-1} (m); elemental analysis calcd (%) for $C_9H_{24}N_3P_3O_{10}ClTb\cdot 3H_2O$: C 16.00, H 4.48, N 6.22; found: C 16.02, H 4.39, N 6.19; thermal analysis shows that the weight loss in the 50–143 °C temperature range is 10.3%, close to the calculated value for the release of four water molecules (10.7%).

$[Eu\{C_9N_3H_{20}(PO_3H)_2(PO_3)\}(H_2O)]ClO_4\cdot 8H_2O$ (3Eu): A solution of $notpH_6$ (0.05 mmol, 0.020 g) in water (10 mL) was added to a solution of $Eu(ClO_4)_3\cdot 6H_2O$ (0.05 mmol, 0.028 g) in water (5 mL). $HClO_4$ (1 M) was dropped into the mixture until the solution became clear (pH ≈ 1.5). The clear solution was left at room temperature for a week to afford colorless prismatic crystals of **3Eu** in a yield of 68% based on $notpH_6$. IR (KBr): $\tilde{\nu}$ = 3421–2866 (br), 1637 (m), 1496 (w), 1458 (w), 1107 (s), 938 (m), 774 (w), 742 (w), 626 (m), 553 cm^{-1}(m); elemental analysis calcd (%) for $C_9H_{24}N_3P_3O_{14}ClEu\cdot 8H_2O$: C 13.14, H 4.90, N 5.11; found: C 13.21, H 4.86, N 5.24; thermal analysis shows a weight loss of 20.5% in the 50–180 °C temperature range, close to the calculated value for the release of nine water molecules (19.6%).

$[Gd\{C_9N_3H_{20}(PO_3H)_2(PO_3)\}(H_2O)]ClO_4\cdot 8H_2O$ (3Gd): The preparation of this compound follows the same procedure as for **3Eu** except that $Gd(ClO_4)_3$ (0.05 mmol, 0.028 g) was used as the starting material instead of $Eu(ClO_4)_3$. The pH of the reaction mixture is about 1.6. The colorless prismatic crystals of **3Gd** were obtained in a yield of 61% based on $notpH_6$. IR (KBr): $\tilde{\nu}$ = 3415–2865 (br), 1637 (w), 1496 (w), 1458 (w), 1120 (s), 1090 (s), 938 (m), 770 (w), 744 (w), 627 (m), 552 cm^{-1}(m); elemental analysis calcd (%) for $C_9H_{24}N_3P_3O_{14}ClGd\cdot 8H_2O$: C 13.05, H 4.87, N 5.07; found: C 13.11, H 4.72, N 5.05; thermal analysis shows a weight loss of 21.1% in the 50–180 °C temperature range, which is slightly

 © 2007 Wiley-VCH Verlag GmbH & Co. KGaA, Weinheim

higher than the calculated value for the release of nine water molecules (19.6%).

[Gd{$C_9N_3H_{20}(PO_3H)_2(PO_3)$}$(H_2O)$]$ClO_4$·3$H_2O$ (4Gd): A solution of notpH_6 (0.05 mmol, 0.020 g) in water (10 mL) was added to a solution of $Gd(ClO_4)_3$·6H_2O (0.05 mmol, 0.028 g) in water (5 mL). $HClO_4$ (1 M) was dropped into the mixture until pH≈1.1. The clear solution was left at room temperature for 2 weeks to afford colorless prismatic crystals of **4Gd** in a yield of 75% based on notpH_6. IR (KBr): $\tilde{\nu}$ = 3440–2920 (br), 1637 (m), 1459 (w), 1120 (s), 1107 (s), 929 (w), 769 (w), 737 (w), 626 (m), 566 cm^{-1}(w); elemental analysis calcd (%) for $C_9H_{24}N_3P_3O_{14}ClGd$·3$H_2O$: C 14.65, H 4.10, N 5.69; found: C 13.78, H 3.87, N 5.60; thermal analysis shows that the weight loss in the 50–150 °C temperature range is 9.6%, close to the calculated value for the release of four water molecules (10.0%). Between 150 °C and 220 °C, a plateau is observed in the TG curve, suggesting that the framework structure is maintained after the removal of both the lattice and coordinated water molecules. XRD measurements confirmed this result.

[Tb{$C_9N_3H_{20}(PO_3H)_2(PO_3)$}$(H_2O)$]$ClO_4$·3$H_2O$ (4Tb): Drops of 1 M $HClO_4$ were added to a solution of notpH_6 (0.05 mmol, 0.020 g) and Tb$(ClO_4)_3$·6H_2O (0.05 mmol, 0.028 g) in water (15 mL) until the mixture became clear (pH≈1.4). The clear solution was left for a week at room temperature to afford colorless prismatic crystals of **4Tb** in 80% yield. IR (KBr): $\tilde{\nu}$ = 3447–2867 (br), 1637 (m), 1497 (w), 1459 (w), 1431 (w), 1150 (s), 1108 (s), 929 (w), 773 (w), 738 (w), 626 (w), 570 cm^{-1} (w); elemental analysis calcd (%) for $C_9H_{24}N_3P_3O_{14}ClTb$·3$H_2O$: C 14.61, H 4.09, N 5.68; found: C 14.09, H 4.03, N 5.78; thermal analysis shows a weight loss of 10.4% in the 50–150 °C temperature range, close to the calculated value for the release of four water molecules (10.0%).

Crystallographic analyses: Data collection for complexes **1Gd**, **2Gd**, **3Eu**, **4Gd**, and **4Tb** was carried out on a Bruker SMART APEX CCD diffractometer equipped with graphite monochromated $Mo_{K\alpha}$ (λ = 0.71073 Å) radiation at 298 K. A hemisphere of data was collected in the θ range of 3.06–25.0° for **1Gd**, 1.94–25.0° for **2Gd**, 0.97–26.0° for **3Eu**, 2.27–26.0° for **4Gd**, and 2.28–26.0° for **4Tb**, using a narrow-frame method with scan widths of 0.30° in ω and an exposure time of 10 s per frame. The data were integrated using the Siemens SAINT program,[20] with the intensities corrected for Lorentz factor, polarization, air absorption, and absorption due to variation in the path length through the detector faceplate. Empirical absorption and extinction corrections were applied. The structure was solved by direct method and refined on F^2 by full-matrix least squares using SHELXTL.[21] All the non-hydrogen atoms were refined anisotropically. All the hydrogen atoms were put in calculated positions or located from the Fourier maps and refined isotropically with the isotropic vibration parameters related to the non-hydrogen atom to which they are bonded.

CCDC-283019–283023 contain the supplementary crystallographic data for this paper. These data can be obtained free of charge from The Cambridge Crystallographic Data Centre via www.ccdc.cam.ac.uk/data_request/cif.

Acknowledgements

We thank the NNSF of China (No. 20325103) and the Ministry of Education of China for financial support, as well as Mr. Yong-Jiang Liu for crystal data collections and Dr. You Song for magnetic measurements.

[1] a) P. Caravan, J. J. Ellison, T. J. McMurry, R. B. Lauffer, *Chem. Rev.* **1999**, *99*, 2293; b) V. Comblin, D. Gilsoul, M. Hermann, V. Humblet, V. Jacques, M. Mesbahi, C. Sauvage, J. F. Desreux, *Coord. Chem. Rev.* **1999**, *185–186*, 451; c) V. Kubíèek, J. Rudovský, J. Kotek, P. Hermann, L. V. Elst, R. N. Muller, Z. I. Kolar, H. T. Wolterbeek, J. A. Peters, I. Lukeš, *J. Am. Chem. Soc.* **2005**, *127*, 16477; d) Q. Zheng, H.-Q. Dai, M. E. Merritt, C. Malloy, C.-Y. Pan, W.-H. Li, *J. Am. Chem. Soc.* **2005**, *127*, 16178; e) F. Benetollo, G. Bombieri, L. Calabi, S. Aime, M. Botta, *Inorg. Chem.* **2003**, *42*, 148; f) M. Woods, Z. Kovacs, S.-R. Zhang, A. D. Sherry, *Angew. Chem.* **2003**, *115*, 6069; *Angew. Chem. Int. Ed.* **2003**, *42*, 5889; g) S. Aime, M. Botta, G. Cravotto, L. Frullano, G. B. Giovenzana, S. G. Crich, G. Palmisano, M. Sisti, *Helv. Chim. Acta* **2005**, *88*, 588; h) J. Paris, C. Gameiro, V. Humblet, P. K. Mohapatra, V. Jacques, J. F. Desreux, *Inorg. Chem.* **2006**, *45*, 5092; i) S. Aime, L. Calabi, C. Cavallotti, E. Gianolio, G. B. Giovenzana, P. Losi, A. Maiocchi, G. Palmisano, M Sisti, *Inorg. Chem.* **2004**, *43*, 7588.

[2] a) W.-S. Liu, T.-Q. Jiao, Y.-Z. Li, Q.-Z. Liu, M.-Y. Tan, H. Wang, L.-F. Wang, *J. Am. Chem. Soc.* **2004**, *126*, 2280; b) R. Ziessel, L. J. Charbonnière, *J. Alloys Compd.* **2004**, *374*, 283; c) M. Vicente, R. Bastida, C. Lodeiro, A. Macías, A. J. Parola, L. Valencia, S. E. Spey, *Inorg. Chem.* **2003**, *42*, 6768; d) T. Gunnlaugsson, C. P. McCoy, F. Stomeo, *Tetrahedron Lett.* **2004**, *45*, 8403.

[3] a) H. C. Aspinall, *Chem. Rev.* **2002**, *102*, 1807; b) R. S. Dickins, S. Gaillard, S. P. Hughes, A. Badari, *Chirality* **2005**, *17*, 357; c) T. Gunnlaugsson, R. J. H. Davies, P. E. Kruger, P. Jensen, T. McCabe, S. Mulready, J. E. O'Brien, C. S. Stevensonb, A.-M. Fanninga, *Tetrahedron Lett.* **2005**, *46*, 3761.

[4] a) K. P. Wainwright, *Coord. Chem. Rev.* **1997**, *166*, 35; b) J. Costamagna, G. Ferraudi, B. Matsuhiro, M. Campos-Vallette, J. Canales, M. Villagran, J. Vargas, M. J. Aguirre, *Coord. Chem. Rev.* **2000**, *196*, 125.

[5] I. Lukes, J. Kotek, P. Vojtisek, P. Hermann, *Coord. Chem. Rev.* **2001**, *216–217*, 287.

[6] J. Huskens, A. D. Sherry, *J. Am. Chem. Soc.* **1996**, *118*, 4396.

[7] M. Yu. Antipin, A. P. Baranov, M. I. Kabachnik, T. Ya Medved, Yu. M. Polikarpov, Yu. T. Struchkov, B. K. Shcherbakov, *Dokl. Akad. Nauk SSSR* **1986**, *287*, 130.

[8] M. I. Kabachnik, M. Yu Antipin, B. K. Shcherbakov, A. P. Baranov, Yu. T. Struchkov, T. Ya Medved, Yu. M. Polikarpov, *Koord. Khim.* **1988**, *14*, 536.

[9] S.-S. Bao, G.-S. Chen, Y. Wang, Y.-Z. Li, L.-M. Zheng, Q.-H. Luo, *Inorg. Chem.* **2006**, *45*, 1124.

[10] C. Geraldes, R. D. Brown, W. P. Cacheris, S. H. Koenig, A. D. Sherry, M. Spiller, *Magn. Reson. Med.* **1989**, *9*, 94.

[11] a) A. S. Craig, D. Parker, H. Adams, N. A. Bailey, *Chem. Commun.* **1989**, 1793; b) D. A. Moore, P. E. Fanwick, M. J. Welch, *Inorg. Chem.* **1990**, *29*, 672; c) C. J. Broan, J. P. L. Cox, A. S. Craig, R. Kataky, D. Parker, A. Harrison, A. M. Randall, G. Ferguson, *J. Chem. Soc. Perkin Trans. 1* **1991**, 87; d) A. Jyo, T. Kohno, Y. Terazono, S. Kawano, *Anal. Sci.* **1990**, *6*, 323.

[12] a) Y. J. Kim, M. Suh, D.-Y. Jung, *Inorg. Chem.* **2004**, *43*, 245; b) J. Rohovec, P. Vojtisek, P. Hermann, J. Mosinger, Z. Zak, I. Lukes, *J. Chem. Soc. Dalton Trans.* **1999**, 3585; c) B. Zhao, X.-Y. Chen, P. Cheng, D.-Z. Liao, S.-P. Yan, Z.-H. Jiang, *J. Am. Chem. Soc.* **2004**, *126*, 15394.

[13] O. Kahn, *Molecular Magnetism*, VCH, New York, **1993**.

[14] A. Rohde, S. T. Hatscher, W. Urland, *J. Alloys Compounds* **2004**, *374*, 137.

[15] a) P. Biginelli, *Gazz. Chim. Ital.* **1893**, *23*, 360; b) C. O. Kappe, *Acc. Chem. Res.* **2000**, *33*, 879; c) M. J. Lusch, J. A. Tallarico, *Org. Lett.* **2004**, *6*, 3237.

[16] a) K. S. Atwal, B. N. Swanson, S. E. Unger, D. M. Floyd, S. Moreland, A. Hedberg, B. C. O'Reilly, *J. Med. Chem.* **1991**, *34*, 806; b) C. O. Kappe, *Eur. J. Med. Chem.* **2000**, *35*, 1043; c) C. O. Kappe, *QSAR Comb. Sci.* **2003**, *22*, 630; d) T. M. Mayer, T. M. Kapoor, S. J. Haggarty, R. W. King, S. L. Schreiber, T. J. Mitchison, *Science* **1999**, *286*, 971; e) Z. D. Aron, L. E. Overman, *Chem. Commun.* **2004**, 253.

[17] a) Y. Ma, C.-T. Qian, L.-M. Wang, M. Yang, *J. Org. Chem.* **2000**, *65*, 3864; b) Y.-J. Huang, F.-Y Yang, C.-J. Zhu, *J. Am. Chem. Soc.* **2005**, *127*, 16386.

[18] Compound **4Gd** (16 mg 0.025 mmol) was added to a solution of benzaldehyde (50 μL, 0.5 mmol), ethyl acetoacetate (65 μL, 0.5 mmol), and thiourea (36 mg, 0.6 mmol) in methanol (2 mL). After the reaction mixture was stirred at room temperature for 48 h, water (5 mL) was added and the product was extracted with ethyl acetate (3×5 mL). After the organic layer was dried with anhydrous Na_2SO_4 and evaporated, the residue was purified by prepared TLC

 © 2007 Wiley-VCH Verlag GmbH & Co. KGaA, Weinheim

(petroleum ether/ethyl acetate 3:1) to afford 5-ethoxycarbonyl-6-methyl-4-phenyl-3,4-dihydropyrimidin-2(1*H*)-one (63 mg) in 60% yield. ^{1}H NMR (300 MHz, DMSO, TMS): δ = 9.18(s, 1H; NH), 7.73(s, 1H; NH), 7.35–7.30(m, 2H; Ar-H), 7.25–7.15(m, 3H; Ar-H), 5.14 (s, 1H; CH), 4.02–3.95 (q, J = 7.1 Hz, 2H; -OCH_2-), 2.24–2.17 (s, 3H; -CH_3), 1.12–1.07 ppm (t, J = 7.1 Hz, 3H; -CH_3); EIMS: m/z: 260.3 [M^+].

[19] a) K. Wieghard, W. Schmid, B. Nuber, J. Weiss, *Chem. Ber.* **1979**, *112*, 2220; b) T. J. Atkins, J. E. Richman, W. F. Oettle, *Org. Synth.* **1978**, *58*, 87.

[20] SAINT, Program for Data Extraction and Reduction, Siemens Analytical X-ray Instruments, Madison, WI, **1994–1996**.

[21] SHELXTL (version 5.0), Reference Manual, Siemens Industrial Automation, Analytical Instruments, Madison, WI, 1**995**.

Received: July 28, 2006
Published online: December 15, 2006

 © 2007 Wiley-VCH Verlag GmbH & Co. KGaA, Weinheim